PHYSICAL REVIEW A VOLUME 27, NUMBER 4 APRIL 1983

Forced Rayleigh scattering: Thermal and acoustic effects in phase-conjugate wave-front generation

Rashmi C. Desai,* M. D. Levenson, and J. A. Barker
IBM Research Laboratory, San Jose, California 95193
(Received 9 July 1982)

We present and discuss a theory for hydrodynamic effects in forced-Rayleigh-scattering experiments. The efficiency of phase-conjugate wave-front generation by forced Rayleigh scattering varies significantly with the nature of the solvent and the scattering angle. Acoustic effects become important for small scattering angles and times shorter than 0.5 ns under which conditions the simple thermal-diffusion theory fails. The phase-conjugate reflection efficiency predicted by our theory at short times is much smaller than that predicted by the thermal-diffusion theory, and thus need not obscure other quantum electronic processes.

I. INTRODUCTION

When mutually coherent laser beams cross in an absorbing medium, an interference pattern is formed which is capable of heating the medium nonuniformly. One result of this nonuniform heating is a grating of refractive-index variations that can Bragg-scatter a third beam. Since the refractive-index variations in the steady state are proportional to the temperature fluctuations induced by the crossing beams, this phenomenon has been termed "forced Rayleigh scattering" and has been used to measure thermal conductivities and coefficients of elasticity in liquid, solid, and liquid-crystal media.[1]

When the third beam has the same wavelength as the initial two and propagates in a direction opposite one of them, the scattered beam propagates back in the direction opposite to the remaining beam. This scattered wave is termed a "phase-conjugate" replica of the initial object beam because its wave fronts match those of the object beam exactly except that the sign of the time appears reversed. Thus forced Rayleigh scattering can generate conjugate wave fronts in a manner analogous to saturation, the Kerr effect, and the other phenomena of degenerate four-wave mixing.[2–4] It has sometimes proved experimentally difficult to separate the effects of forced Rayleigh scattering from those due to quantum electronic phenomena of greater physical or chemical interest.[5] Recent experimental results have demonstrated that high conjugate wave-front generation efficiencies can be achieved in media where only the forced Rayleigh mechanism is significant.[6] These experiments utilize short laser pulses and operate in a transient time regime incompletely described by the standard thermal model.[3] We have performed a full hydrodynamical calculation including the effects of sound waves as well as thermal diffusion on the amplitude of the scattered conjugate wave. These calculations confirm the validity of the standard model for time scales longer than 1 or 2 ns. However, our results indicate that the thermal model breaks down completely for times shorter than 0.1 ns and that a number of interesting phenomena then occur.

The physical interpretation of the effects revealed by the hydrodynamic calculation is fairly simple. The index-of-refraction grating which scatters the conjugate wave in the steady state results mostly from variations in the density of the medium. Since these density variations result from a nonuniform *heating*, their presence implies that differential expansion of the most strongly heated parts of the medium has taken place. However, in the initial few picoseconds after the energy has been deposited, the medium has not yet had time to expand. The density is thus constant, and any index change is due to the intrinsic variation in the index of refraction with temperature at constant density. Subsequently, sound waves produced by the nonuniform heating propagate across the medium and begin the expansion process. The propagation of these pressure-density waves gives rise to an oscillating refractive-index variation and an oscillating reflection efficiency. Finally, the sound waves damp out, and the usual thermal-diffusion mode becomes dominant. Only in this final time regime (the onset of which occurs in roughly 1 ns) is the usual model adequate. Our results imply that other nonlinear optical phenomena can be experimentally separated from forced-

Rayleigh-scattering effects by performing experiments in the shortest possible time interval.

Earlier discussions of oscillatory reflection efficiencies in four-wave mixing concentrated on effects unique to absorbing molecular crystals.[7] Our calculations are based on a model in which only the index of refraction and hydrodynamics of the transparent host material matters. The absorbing species is assumed to deposit the optical energy as heat in the medium in a time short in comparison to all other time scales in the process and thereafter to have no effect upon the scattering. Such an approximation is valid for many media when the absorption depth of the medium is many times larger than the grating spacing. The time evolution of the oscillations predicted by our model differs markedly from those reported in molecular crystals. While the effects predicted by our calculations have not yet been directly observed, the known parameters of a number of solvent-dye systems imply that they can be observed and exploited scientifically.

II. CALCULATIONS

A. Electrodynamics

Conjugate wave-front generation by forced Rayleigh scattering can be divided into two stages when the two pump beams are mutually incoherent. In the first stage, an object beam $E_0(\vec{r},t)$ interferes with the forward propagating pump beam $E_1(\vec{r},t)$ to write a grating of index-of-refraction variations in the medium. In the second stage, this index grating scatters the second pump beam $[E_2(\vec{r},t)]$ into a beam which propagates as the phase conjugate of the object beam and which is characterized by the electric field $E_s(\vec{r},t)$.[3,8] Since this paper emphasizes the dynamics of the index grating, we shall simplify the electrodynamics of grating writing and scattering as much as consistency allows.

A typical wave-front conjugation geometry is modeled in Fig. 1. The electric fields have the form

$$E_j(\vec{r},t)=\tfrac{1}{2}\mathscr{E}_j(\vec{r},t)e^{i(\vec{k}_j\cdot\vec{r}-\omega t)}+\text{c.c.} \tag{1}$$

The object wave propagates in the negative direction along the z axis with amplitude $\mathscr{E}_0(\vec{r},t)$ and wave vector $\vec{k}_0=-(n_0\omega/c)\hat{z}=-k\hat{z}$. The forward pump beam has amplitude $\mathscr{E}_1(\vec{r},t)$ and wave vector

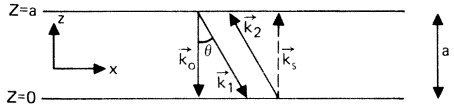

FIG. 1. Geometry of the four-wave-mixing experiment considered in the paper.

$\vec{k}_1=-k(\hat{z}\cos\theta-\hat{x}\sin\theta)$. The medium has an unperturbed index of refraction of n_0 and a constant absorption constant β. Inside the medium, the object and initial pump amplitudes obey the equations

$$\frac{d\mathscr{E}_o}{dz}-\frac{\beta}{2}\mathscr{E}_o=i\kappa_q\mathscr{E}_1-i\kappa_0\mathscr{E}_o\ , \tag{2}$$

$$\cos\theta\frac{d\mathscr{E}_1}{dz}-\frac{\beta}{2}\mathscr{E}_1=i\kappa_q^*\mathscr{E}_o-i\kappa_0\mathscr{E}_1\ , \tag{3}$$

where the parameters

$$\kappa_q(\vec{r},t)=\frac{\omega\,\delta n_q(\vec{r},t)}{c}\ ,\qquad \kappa_0(\vec{r},t)=\frac{\delta n_0(\vec{r},t)\omega}{c}\ , \tag{4}$$

describe the coupling due to the sinusoidal index-of-refraction variation

$$n(\vec{r},t)=n_0+[\tfrac{1}{2}\delta n_q(\vec{r},t)e^{i\vec{q}\cdot\vec{r}}+\text{c.c.}]+\delta n_0(\vec{r},t) \tag{5}$$

with amplitude $\delta n_q(\vec{r},t)$ and grating wave vector $\vec{q}$, and the nonoscillatory change δn_0 which results in thermal defocusing. The waves fulfill the boundary conditions

$$\mathscr{E}_o(z=a,t)=\begin{cases}A_0\ , & 0<t<t_p\\ 0\ , & \text{otherwise}\end{cases}$$
$$\mathscr{E}_1(z=a,t)=\begin{cases}A_1\ , & 0<t<t_p\\ 0\ , & \text{otherwise}\end{cases} \tag{6}$$

at the plane $z=a$ which bounds the nonlinear medium. The laser pulse length is t_p.

The two waves form an interference pattern in the medium. The light intensity varies as

$$\delta I_q(\vec{r},t)=\frac{nc}{8\pi}(\mathscr{E}_0^*\mathscr{E}_1e^{i\vec{q}\cdot\vec{r}}+\mathscr{E}_0\mathscr{E}_1^*e^{-i\vec{q}\cdot\vec{r}})\ , \tag{7}$$

where $\vec{q}=\vec{k}_0-\vec{k}_1$ is the characteristic wave vector of the resulting grating and $|\vec{q}|=q=2k\sin(\theta/2)$. The light absorbed by the medium is converted to heat, and the spatially oscillating part of the intensity gives rise to a spatially oscillating heat production per unit volume

$$\delta Q_q(\vec{r},t)=\beta\,\delta I_q(\vec{r},t)\ . \tag{8}$$

This heat production produces the index-of-refraction variation which couples the waves and scatters the conjugate wave front. A similar term proportional to the average light intensity leads to the index change $\delta n_0(\vec{r},t)$.

Because the index of refraction does not instantaneously respond to changes in the heat flux, it is not possible to solve Eqs. (2) and (3) except by numerical methods. For sufficiently weak amplitudes, one can ignore the coupling between the forward pump and object beams and set the right-hand side of Eq. (2) to zero. This assumption facilitates analytical solution; however, it introduces errors in the description of wave-front conjugation that becomes significant whenever the theoretical efficiency exceeds a few percent.[4]

The backwards pump beam propagates through the medium with wave vector $\vec{k}_2=-\vec{k}_1$. With the undepleted pump approximation its electric field amplitude is described by

$$\mathscr{E}_2(\vec{r},z)=\begin{cases}A_2(t)\exp\dfrac{-\beta z}{2\cos\theta}\ , & t_d<t<t_p+t_d\ ,\quad \theta\neq 90^\circ\\ 0\ , & \text{otherwise}\end{cases} \tag{9}$$

where t_d is the delay of the backwards propagating pulse. It is convenient to assume that this wave is *incoherent* with the object and first pump wave. In this case, only one grating—the grating with wave vector $\vec{q}$—mediates the wave-front conjugation process, and some of the mode-coupling effects that complicate many other treatments of four-wave mixing can be ignored.[4,8,9] It is also assumed that the interference between the backward pump and phase-conjugate beam makes no contribution to the index grating.

The bulk of this paper concerns the time evolution of the index-of-refraction grating which results from the deposition of heat in the medium. The spatially oscillating part of the index of refraction is assumed to have a negligible imaginary part ($\delta\beta \ll k\,\delta n$). The spatial oscillations in the index of refraction scatter the second pump wave, giving rise to the phase-conjugate beam which propagates with wave vector $k_s=-k_0$. The electric field amplitude of the phase-conjugate signal wave obeys

$$\frac{d}{dz}\mathscr{E}_s+\frac{\beta}{2}\mathscr{E}_s=-i\kappa_q^*(\vec{r},t)\mathscr{E}_2(\vec{r})\ , \tag{10}$$

where $\mathscr{E}_s(z=0)\equiv 0$, and the interaction region is assumed small enough that retardation effects can be ignored (i.e., $a<ct_p$).

The solution to Eq. (9) which described the amplitude leaving the medium is then

$$\mathscr{E}_s(a,t)=\begin{cases}-ip^{1/2}(\cos\theta)A_2\delta n_q(t)\ , & t_d<t<t_p+t_d\\ 0\ , & \text{otherwise}\end{cases} \tag{11}$$

where $p(\cos\theta)=\omega^2 e^{-\beta a/\cos\theta}(1-e^{-\beta a})^2/\beta^2c^2$, and the intensity in the conjugate wave is

$$I_s(a,t)=\frac{nc}{4\pi}\,|\,\mathscr{E}_s(a,t)\,|^2 \tag{12}$$

in cgs units.

Two efficiencies can be defined for this wave-front conjugation process. The phase-conjugate reflection efficiency

$$\eta_\phi(t_p,t_d)=\frac{\displaystyle\int_{t_d}^{t_d+t_p}|\,\mathscr{E}_s(z=a,t)\,|^2dt}{\displaystyle\int_0^{t_p}|\,\mathscr{E}_o(z=a,t)\,|^2dt} \tag{13}$$

gives the ratio of the conjugate wave intensity to the object wave intensity.[4] If $\eta_\phi>1$, the wave-front conjugator is said to act as a phase-conjugate mirror with gain. The Bragg-scattering efficiency relates the phase-conjugate wave to the backwards pump intensity[1]

$$\eta_\beta(t_p,t_d)=\frac{\displaystyle\int_{t_d}^{t_d+t_p}|\,\mathscr{E}_s(z=a,t)\,|^2dt}{\displaystyle\int_{t_d}^{t_d+t_p}|\,\mathscr{E}_2(z=0,t)\,|^2dt}$$

$$=\frac{A_0^2}{A_2^2}\eta_\phi(t_p,t_d)\ . \tag{14}$$

The Bragg efficiency is the quantity usually measured in forced-Rayleigh-scattering experiments and cannot exceed unity. The terms neglected on the right-hand side of Eq. (2) are proportional to $[\eta_\beta(t_p,0)]^{1/2}$. Thus the present analysis is correct only for $\eta_\beta(t_p,0)\ll 1$.

For simpler discussion, it is convenient to define a single figure of merit equal to the efficiency for unit input intensities

$$F(\cos\theta,t_p,t_d)=\frac{\eta_\phi(t_p,t_d)}{I_1^0I_2^0}=\frac{\eta_\beta(t_p,t_d)}{I_0^0I_1^0}\ , \tag{15}$$

where $I_j^0=(nc/4\pi)A_j^2$. A related quantity which depends only upon the hydrodynamic parameters of the solvent is defined in Eq. (24).

B. Refractive-index fluctuation and hydrodynamics

As shown above in Sec. II A, theoretical computation of the image wave intensity $I_s(t)$ and the phase-conjugate reflectivity F or the conjugation efficiency η_ϕ requires the knowledge of the refractive-index fluctuation $\delta n_q(t)$ at wave vector $\vec{q}$. To obtain $\delta n_q(t)$, we first express it in terms of the density and temperature fluctuations in the medium

$$\delta n_q(t)=\left[\frac{\partial n}{\partial \rho}\right]_T \rho_q(t)+\left[\frac{\partial n}{\partial T}\right]_\rho T_q(t)\ , \tag{16}$$

where $\rho_q(t)$ and $T_q(t)$ are the amplitudes of small sinusoidally varying components of density and temperature, respectively. Typically, the fluid medium used to generate the phase-conjugate wave would have a solventlike cyclohexane as well as some absorber, e.g., α-napthyl-phenyl-oxazole (α-NPO). We assume that the only effect the absorbing species has is to deposit the absorbed laser-beam energy uniformly in the medium. Thus we treat the fluid medium in which the thermal grating is created as essentially a one-component system insofar as the evaluation of $\delta n_q(t)$ is concerned. To obtain $\rho_q(t)$ and $T_q(t)$, we use the equations of linear hydrodynamics in which the temperature equation has a source term at wave vector $\vec{q}$ as is physically required for the phenomena of forced Rayleigh scattering [see Eq. (8)].[10–12] Such a set of hydrodynamic equations is given below for the variables $\rho_k(t)$, $\psi_k(t)$, and $T_k(t)$; since only the longitudinal part of local fluid velocity $\vec{v}$ enters the equations, we use the velocity variable $\psi_q \equiv i\vec{q}\cdot\vec{v}$. The equations are the continuity equation

$$\frac{\partial \rho_k(t)}{\partial t}+\rho_0\psi_k(t)=0\ , \tag{17a}$$

the Navier-Stokes equation

$$\rho_0\frac{\partial \psi_k(t)}{\partial t}+(\tfrac{4}{3}\eta+\zeta)k^2\psi_k(t) - \left[\frac{\partial p}{\partial T}\right]_\rho k^2 T_k(t)-\left[\frac{\partial p}{\partial \rho}\right]_T k^2\rho_k(t)=0\ , \tag{17b}$$

and the thermal-diffusion equation

$$\rho_0 C_v\frac{\partial T_k(t)}{\partial t}+T_0\left[\frac{\partial p}{\partial T}\right]_\rho \psi_k(t)+\kappa k^2 T_k(t) =\beta\frac{nc}{8\pi}\mathscr{E}_0(t)\mathscr{E}_1(t)\delta(\vec{k}-\vec{q})\ . \tag{17c}$$

In the above equations, η,ζ,κ are the thermal transport coefficients of shear viscosity, bulk viscosity, and thermal conductivity, respectively; the equation of state for pressure $p=p(\rho,T)$ has to be used to obtain the thermodynamic derivatives $(\partial p/\partial\rho)_T$ and $(\partial p/\partial T)_\rho$ and C_v is the specific heat at constant volume. The solution of these hydrodynamic equations also involves (i) the specific heat at constant pressure C_p through the thermodynamic identity

$$C_p=C_v+\left[\left[\frac{\partial p}{\partial T}\right]_\rho\right]^2\Big/\left[\rho_0\left[\frac{\partial p}{\partial \rho}\right]_T\right] \tag{18}$$

and (ii) the adiabatic sound speed $c_0=[\gamma(\partial p/\partial\rho)_T]^{1/2}$, where $\gamma=C_p/C_v$. In writing the right-hand side (rhs) of Eq. (17c), we have used Eq. (8) for the heat production rate from the thermal grating.

In obtaining the solution to Eq. (17), appropriate to the phenomena of forced Rayleigh scattering, we assume that the forcing source term, rhs of Eq. (17c) is dominant over the initial thermal fluctuations $\rho_k(0)$, $\psi_k(0)$, and $T_k(0)$ and ignore the latter. With these assumptions, we have exactly solved the hydrodynamic equations for $\rho_q(t)$ and $T_q(t)$. Using Eq. (16), we can express the result for the refractive-index fluctuation $\delta n_q(t)$ in terms of the hydrodynamic Green's function $G(q,t)$ as

$$\delta n_q(t)=\beta\frac{nc}{8\pi}\int_0^t G(q,t')\mathscr{E}_0(t-t')\mathscr{E}_1(t-t')dt'\ , \tag{19a}$$

where

$$G(q,t)=\frac{\lambda\alpha_1^2-\mu\alpha_1+\nu}{(\alpha_1-\alpha_2)(\alpha_1-\alpha_3)}e^{-\alpha_1 t} +\frac{\lambda\alpha_2^2-\mu\alpha_2+\nu}{(\alpha_2-\alpha_1)(\alpha_2-\alpha_3)}e^{-\alpha_2 t} +\frac{\lambda\alpha_3^2-\mu\alpha_3+\nu}{(\alpha_3-\alpha_1)(\alpha_3-\alpha_2)}e^{-\alpha_3 t}\ . \tag{19b}$$

In Eq. (19), $\lambda=(\partial n/\partial T)_\rho$, $\mu=(\partial n/\partial T)_\rho D_v q^2$, and $\nu=(\partial p/\partial\rho)_T(\partial n/\partial T)_\rho q^2$ with $D_v=(\frac{4}{3}\eta+\zeta)\rho^{-1}$ as the kinematic longitudinal viscosity and $(\partial n/\partial T)_p=(\partial n/\partial T)_\rho+(\partial n/\partial\rho)_T(\partial\rho/\partial T)_p$. In the usual approximate theory of forced Rayleigh scattering—which we discuss in Sec. II C—an assumption of neglecting $(\partial n/\partial T)_\rho$ (and hence λ and μ) is made.[1,3] Equation (19) also contains α_1, α_2, and α_3 which are the complex decay constants of the q-dependent hydrodynamic modes and are the solutions of the cubic dispersion relation

$$[z^3+z^2(D_v+\gamma D_T)q^2+z(c_0^2q^2+\gamma D_T D_v q^4)+(c_0^2 D_T q^4)]\equiv[(z+\alpha_1)(z+\alpha_2)(z+\alpha_3)]=0\ . \tag{20}$$

Even though we use the full solution to the cubic equation, to obtain $\alpha_1,\alpha_2,\alpha_3$, it is useful to note that in the range of wave vectors ($q\lesssim 5\times10^5$ cm^{-1}) encountered in the forced-Rayleigh-scattering experiments, the small-q solution is quite accurate. For small q one gets

$$\alpha_1 = -ic_0 q + \Gamma q^2 + O(q^3) ,$$
$$\alpha_2 = +ic_0 q + \Gamma q^2 + O(q^3) , \tag{21}$$

and

$$\alpha_3 = D_T q^2 + O(q^3) ,$$

where $\Gamma = \frac{1}{2}[D_v + D_T(\gamma - 1)]$ with $D_T = \kappa/(\rho C_p)$. Thus the pair of complex-conjugate roots α_1, α_2 is the acoustic modes, and α_3 is the thermal-diffusion mode. Owing to the propagating nature of α_1, α_2, the terms involving $e^{-\alpha_1 t}$ and $e^{-\alpha_2 t}$ in Eq. (19) lead to damped oscillatory behavior for the solution. Since $\alpha_2 = \alpha_1^*$, we introduce the quantities $\mathscr{C}_1, \mathscr{C}_1^*, \mathscr{C}_3$ and rewrite Eq. (19b) as

$$G(q,t) = \alpha_1 \mathscr{C}_1 e^{-\alpha_1 t} + \alpha_1^* \mathscr{C}_1^* e^{-\alpha_1^* t} + \alpha_3 \mathscr{C}_3 e^{-\alpha_3 t} . \tag{19b'}$$

From Eqs. (19a), (19b'), and (6) we obtain the result for the refractive-index fluctuation $\delta n_q(t)$ as

$$\delta n_q(t) = \begin{cases} \dfrac{\beta n c}{8\pi} \dfrac{A_0 A_1}{\rho_0 C_v} \{ 2\,\mathrm{Re}[\mathscr{C}_1 (1 - e^{-\alpha_1 t})] + \mathscr{C}_3 (1 - e^{-\alpha_3 t}) \} , & \text{if } t < t_p \quad (22) \\ \dfrac{\beta n c}{8\pi} \dfrac{A_0 A_1}{\rho_0 C_v} \{ 2\,\mathrm{Re}[\mathscr{C}_1 e^{-\alpha_1 t} (e^{\alpha_1 t_p} - 1)] + \mathscr{C}_3 e^{-\alpha_3 t} (e^{\alpha_3 t_p} - 1) \} , & \text{if } t > t_p . \quad (23) \end{cases}$$

This solution can be substituted in Eq. (11) for scattered field $\mathscr{E}_s(a,t)$, and then the use of Eq. (13) would lead to the result for the phase-conjugate reflection efficiency η_ϕ. For arbitrary values of t_d and t_p, the result is quite complex. The quantity η_ϕ is proportional to $I_1^0 I_0^0$, the product of incident pump and object wave identities ($I_i^0 = nc A_i^2/4\pi$). It is also proportional to the angle-dependent quantity $p(\cos\theta)$ defined in Eq. (11). The hydrodynamic aspects enter η_ϕ through $\delta n_q(t)$, and to highlight these we define a new figure of merit $F_h(\cos\theta, t_p, t_d)$ and write the figure of merit of Eq. (15) as

$$F(\cos\theta, t_p, t_d) = p(\cos\theta) F_h(\cos\theta, t_p, t_d) . \tag{24}$$

The parameter F_h isolates the purely hydrodynamic part in the figure of merit. In Sec. III, we show typical results for F_h for the case with no delay between two pump beams: $t_d = 0$. Even in this limit, the expression for F_h is involved,

$$F_h(\cos\theta, t_p, t_d = 0) = \frac{1}{(\rho_0 C_v)^2} \left[\mathscr{C}_0^2 - 2\mathscr{C}_0 \mathscr{C}_3 \frac{(1 - e^{-\alpha_3 t_p})}{\alpha_3 t_p} + \mathscr{C}_3^2 \frac{(1 - e^{-2\alpha_3 t_p})}{2\alpha_3 t_p} + 2\mathscr{C}_1 \mathscr{C}_1^* \frac{(1 - e^{-(\alpha_1 + \alpha_1^*) t_p})}{(\alpha_1 + \alpha_1^*) t_p} \right.$$
$$+ 2\,\mathrm{Re} \left[\mathscr{C}_1^2 \frac{(1 - e^{-2\alpha_1 t_p})}{2\alpha_1 t_p} - 2\mathscr{C}_0 \mathscr{C}_1 \frac{(1 - e^{-\alpha_1 t_p})}{\alpha_1 t_p} \right.$$
$$\left. \left. + 2\mathscr{C}_1 \mathscr{C}_3 \frac{(1 - e^{-(\alpha_1 + \alpha_3) t_p})}{(\alpha_1 + \alpha_3) t_p} \right] \right] , \tag{25}$$

where $\alpha_1, \alpha_2 = \alpha_1^*, \alpha_3$ are defined in Eq. (20); $\mathscr{C}_1, \mathscr{C}_3$ are defined in Eqs. (19b), (19b'), and

$$\mathscr{C}_0 = \left[\frac{\partial n}{\partial T} \right]_p \Big/ (D_T \gamma q^2) . \tag{25'}$$

The angle dependence of F_h results from the dependence of α_1, α_2, and α_3 upon q. Equation (25) is the central result of this paper. Even though it is a closed algebraic expression, it appears quite complex due to the inclusion of all the three hydrodynamic modes exactly. In Sec. II C, we first look at various approximate limits of this expression in order to understand the importance of different terms in Eq. (25) at various times. There we also discuss the effects of nonzero delay t_d between beams 1 and 2.

C. Limiting behavior and various approximations

In this subsection, we shall consider various limiting behavior and approximate forms of the hydrodynamic Green's function $G(q,t)$, Eq. (19), and the figure of merit F, Eq. (24).

1. Long-time behavior

For most fluids, it is appropriate to ignore the acoustic modes α_1 and α_2 *at long times.* This is because for $q \sim 10^5$ cm^{-1}, typical of optical scattering experiments, $c_0 q > D_T q^2$ [see Eq. (21)]. Also, the variation of refractive index with temperature and density in typical fluid media is such that $(\partial n/\partial T)_\rho$ is small compared to $(\partial n/\partial \rho)_T$ or $(\partial n/\partial \rho)_p$. Thus often it is appropriate to ignore $(\partial n/\partial T)_\rho$ and set λ and μ to zero [see defining equation after Eq. (19)]. These two approximations simplify Eqs. (19) and (25) considerably. The long-time approximation, so constructed, leads to the usual result which takes into account only the thermal-diffusion (TD) mode: One gets

$$G_{\rm TD}(q,t)=\frac{\nu}{(c_0 q)^2}e^{-\alpha_3 t}=\left[\frac{\partial n}{\partial T}\right]_p\frac{C_v}{C_p}e^{-D_T q^2 t} \tag{26}$$

and

$$F_{h,\rm TD}(\cos\theta,t_p)=\left[\frac{1}{\kappa q^2}\left[\frac{\partial n}{\partial T}\right]_p\right]^2\times\left[1+\frac{1}{\alpha_3 t_p}(2e^{-\alpha_3 t_p}-\tfrac{1}{2}e^{-2\alpha_2 t_p}-\tfrac{3}{2})\right], \tag{27}$$

where $\alpha_3 \simeq D_T q^2=\kappa q^2/(\rho C_p)$. This result agrees with the earlier simple theories of thermal grating effects in four-wave-mixing experiments for phase-conjugate reflected-wave generation.[13]

The limiting behavior for large t_p is of the form $(A+B/t_p+\cdots)$. By comparing the formal expansion of exact [Eq. (25)] and approximate [Eq. (27)] expressions for the figure of merit, one can show that Eq. (27) reproduces the constant A correctly, but acoustic modes do make a contribution to the coefficient B. From the numerical computations discussed in Sec. III, we find, however, that this is not significant and the thermal-diffusion approximation is usually quite adequate when t_p is greater than a few nanoseconds.

2. Short-time behavior

On a time scale shorter than a nanosecond, the thermal-diffusion theory, Eq. (27), gives qualitatively incorrect results. For such short times acoustic modes α_1 and α_2 become increasingly more important. The difference becomes apparent on examining the small t_p limit of the exact and approximate expressions in Eqs. (25) and (27), respectively. One gets for small t_p,

$$F(\cos\theta,t_p,0)=p(\cos\theta)\tfrac{1}{3}\left[\left[\frac{\partial n}{\partial T}\right]_\rho\frac{t_p}{\rho_0 C_v}\right]^2+O(t_p^3) \tag{28a}$$

and

$$F_{\rm TD}(\cos\theta,t_p,0)=p(\cos\theta)\tfrac{1}{3}\left[\left[\frac{\partial n}{\partial T}\right]_p\frac{t_p}{\rho_0 C_p}\right]^2+O(t_p^3)\,. \tag{28b}$$

If one ignores the acoustic modes, as in Eq. (28b), one gets constant pressure thermodynamics, whereas correct physics on the short-time scale involves constant density (volume) processes. Numerically, $(\partial n/\partial T)_\rho$ is considerably smaller (often by an order of magnitude) than $(\partial n/\partial T)_p$ for most fluids.[14] Thus the difference between Eqs. (28a) and (28b) would clearly show up in experiments with t_p shorter than 0.1 ns.

3. Intermediate times

For intermediate values of 0.1–2 ns, the effect of acoustic modes is to introduce oscillatory q-dependent behavior in $F(\cos\theta,t_p,0)$. These oscillations are, of course, not present in the thermal-diffusion theory, Eq. (27). Experiments done at small angle θ (and hence small q) should show such effects. In Sec. III, we give some numerical results illustrating the general discussion given above.

4. Delay between pump beams

The general expression for the figure of merit F with $t_d \neq 0$ is quite complex even when the pulse widths of the two pump beams are equal, this being the assumption throughout this paper. So we consider here simpler situations when $t_d \neq 0$. If the pulse width t_p is very small, then one may assume that $\mathscr{E}_s(a,t)$ does not vary significantly during the time interval $t_d \leq t \leq t_d + t_p$. In this case, the result is

$$F_h(\cos\theta,t_d,t_p)=\left[\frac{t_p}{\rho_0 C_v}\right]^2[\,2\,\mathrm{Re}(\alpha_1\mathscr{C}_1 e^{-\alpha_1 t_d})+\alpha_3\mathscr{C}_3 e^{-\alpha_3 t_d}]^2\,, \tag{29}$$

so that F is proportional to the square of the pulse width. This is the regime encountered in many mode-locked laser experiments. If t_p is of the order of a nanosecond or larger, we find (see results of Sec. III) that the thermal-diffusion approximation discussed above is quite good. Within this approximation, the effect of nonzero delay t_d leads to the result

$$F_{h,\mathrm{TD}}(\cos\theta,t_d,t_p)=\begin{cases}\mathscr{C}_3^2 e^{-2\alpha_3(t_d+t_p)}(e^{\alpha_3 t_p}-1)^2(e^{2\alpha_3 t_p}-1)/(2\alpha_3 t_p)\ , & \text{if } t_d>t_p \quad (30a)\\ \mathscr{C}_3^2\left[1-\dfrac{t_d}{t_p}-\dfrac{2}{\alpha_3 t_p}(e^{-\alpha_3 t_d}-e^{-\alpha_3 t_p})\right. & \\ \left.+\dfrac{1}{2\alpha_3 t_p}[(e^{-2\alpha_3 t_d}-e^{-2\alpha_3 t_p})+e^{-2\alpha_3 t_p}(1-e^{-2\alpha_3 t_d})(e^{\alpha_3 t_p}-1)^2]\right]\ , & \text{if } t_d<t_p\ . \quad (30b)\end{cases}$$

If $t_d=0$, Eq. (30b) reduces to Eq. (27), the result of Chiang-Levenson.[13] If $t_d>t_p$, then for very small t_p, Eq. (30a) also yields the result that $F_h\to 0$ as t_p^2, but the coefficient is not correct, and one has to use Eq. (29). If $t_d=t_p$, both Eqs. (30a) and (30b) lead to

$$F_h\to\mathscr{C}_3^2 e^{-2\alpha_3 t_p}(e^{\alpha_3 t_p}-1)^2(1-e^{-2\alpha_3 t_p})/(2\alpha_3 t_p)\ .$$

Thus in order to explore experimentally the effect of delay between the two pump beams on the phase-conjugation efficiency, the simple expressions above may be used as a guide. They also indicate that the maximum efficiency occurs for finite t_d (i.e., $0<t_d<t_p$).

III. RESULTS AND DISCUSSION

In this section, we shall give results of numerical comparison between Eqs. (25) and (27) in order to highlight the acoustic mode effects in forced-Rayleigh-scattering experiments.

Table I gives various constants that we use in the computation; we have studied three typical solvents: water, ethanol, and cyclohexane.[14–16]

In Fig. 2, we show the results for water and ethanol. Also, if (i) we use α-NPO as a typical absorbing species and use $\beta=0.7$ (ii) for a, the cell dimension in z direction, take 1 cm and (iii) assume the wavelength of incident laser beams as 3.55×10^{-5} cm, then the electrodynamic factor $p(\cos\theta)$ becomes $0.8\exp(-0.7/\cos\theta)$ which has the effect of strongly decreasing F [Eq. (25)] as one approaches $\theta=90°$. This is the consequence of the geometry chosen in Fig. 1. (The results for cyclohexane are qualitatively similar to those for ethanol except for the scale—F_h for cyclohexane is about 100 times larger.) The solid lines give the result of including full hydrodynamics as in Eq. (25), and dashed lines are the thermal-diffusion approximation. Various values of t_p used are indicated in the figure. Qualitatively, figure of merit for ethanol is about 100 times larger than for water. For all solvents, the overall magnitude of F_h appears to increase quadratically with t_p in the short-time regime.

When t_p is larger than about 1 ns, thermal-diffusion theory becomes quite accurate at large scattering angles. For shorter times or small angles, the full hydrodynamic theory predicts a phase-conjugate amplitude far below that predicted by the usual thermal-diffusion model. This falloff reflects the difference between constant pressure and constant density processes illustrated in Eq. (28). The time required for the transition between constant density and constant pressure hydrodynamics depends on the wave vector q and hence upon angle. Since $\partial n/\partial T\,|_\rho\neq 0$, the correct figure of merit F_h does not fall to zero at very short times. Still, the effects of forced Rayleigh scattering can be suppressed by choosing to work at the correct angle and time scale. Because $\partial n/\partial T\,|_p$ is relatively small for water, the suppression of F_h at small times is less dramatic in comparison to the peak value than for ethanol and other solvents.

By about 5 ns (results not shown in the figure) the thermal-diffusion approximation becomes quantitatively correct all the way down to scattering angle $\theta\sim 3°$. For $t_p\lesssim 0.5$ ns, thermal-diffusion approximation is unreliable even qualitatively at all angles. For $t_p\approx 1$ ns, and small scattering angles ($\theta\lesssim 30°$),

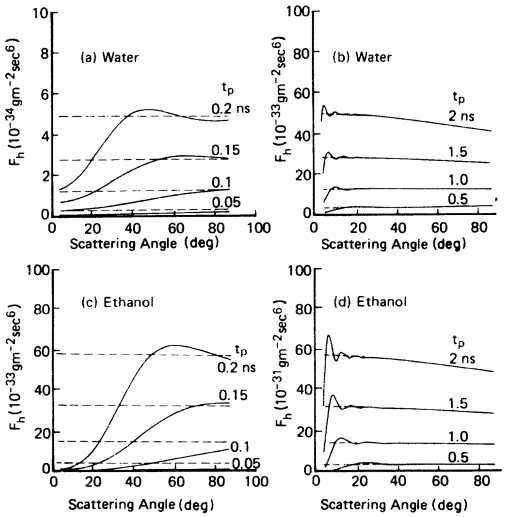

FIG. 2. Hydrodynamic figure of merit F_h: variation with scattering angle and pump beam pulse width t_p. Solid lines, full hydrodynamics [Eq. (25)]; dashed lines, thermal-diffusion approximation [Eq. (27)].

TABLE I. Constants used in numerical computations.

Quantity[a]	Water	Ethanol	Cyclohexane
n_0	1.33	1.361	1.331
$\left[\frac{\partial n}{\partial T}\right]_p$ [(K)$^{-1}$]	-8×10^{-5}	-4×10^{-4}	-5.4×10^{-4}
$\left[\frac{\partial n}{\partial T}\right]_\rho$ [(K)$^{-1}$]	-4×10^{-5}	-3×10^{-5}	-4×10^{-5}
ρ_0(g/cm^3)	0.998	0.789	0.779
C_p[erg/(g K)]	4.18×10^7	2.45×10^7	1.82×10^7
C_v[erg/(g K)]	4.14×10^7	2.11×10^7	1.37×10^7
κ[erg/sec cm K)]	6.04×10^4	1.82×10^4	1.37×10^4
η(poise)	0.98×10^{-2}	1.72×10^{-2}	0.96×10^{-2}
ζ(poise)	2.75×10^{-2}	1.72×10^{-2}	1.5×10^{-2}
c_0(cm/sec)	1.483×10^5	1.162×10^5	1.28×10^5

[a]See text for notations.

one sees interesting oscillatory behavior in F_h (and also in F) from Eq. (25) which arises due to the acoustic interference in the thermal grating which is formed by object and pump waves. Experiments done in this region of θ and t_p should observe these effects. The thermal-diffusion approximation [Eq. (27) and dashed lines in Fig. 2] of course does not have these effects in it. Even though we have not numerically shown effects of varying t_d, the results in Sec. II C are simple enough that they may be useful in experimental analysis.

The forced-Rayleigh-scattering experiments performed to date mostly employ Q-switched laser pulses long enough and angles large enough that the thermal-diffusion model applies rigorously. Many transient grating experiments, however, employ pulses short enough that acoustic propagation effects can dominate the time profile. In the experiments of Salcedo *et al.* and of Nelson and Fayer, the acoustic waves acted primarily to modify the absorption constant of the medium, whereas the present model describes effects resulting from the variation of the real part of the index of refraction.[7] The resulting scattered amplitude is 90° out of phase with the amplitude scattered by absorption gratings, and the variation of the amplitude is qualitatively different from that in Eqs. (11) and (19). The suppression of forced Rayleigh scattering at small angles and for short time may form a "window" useful for investigation of other nonlinear effects. Alternatively, the deviations of the exact hydrodynamic response from that predicted by the thermal-diffusion model can be experimentally detected and used to refine measurements of solvent parameters.

In near-degenerate four-wave-mixing experiments where independent pump and object beam lasers are employed to probe the dynamics of excited-state populations, anomalies due to forced Rayleigh scattering also may appear.[17,18] In these experiments the mutual coherence time of the two pulsed lasers employed is shorter than the pulse length, and thus the average amplitude of the thermal grating is zero $\langle \delta n_q \rangle = 0$. Still, some scattered intensity can result since $I_s \propto \langle (\delta n_q{}^2) \rangle \neq 0$. The theory developed here indicates that the forced-Rayleigh-scattering anomalies on these experiments can be suppressed by the ratio of Eqs. (28a) and (28b) if the mutual coherence time of the lasers (which plays the role of t_p in this case) is short enough and if the angle between object and pump is small enough. This is contrary to the present experimental practice but may be useful in the future.

*Permanent affiliation: Department of Physics, University of Toronto, Toronto, Ontario, Canada M5S 1A7.

[1]D. W. Pohl, IBM J. Res. Dev. 23, 604 (1979), and references therein.

[2]A. Yariv, IEEE J. Quantum Electron. QE-14, 650 (1978); QE-15, 524 (1979), and references therein.

[3]G. Martin and R. W. Hellwarth, Appl. Phys. Lett. 34, 371 (1979).

[4]R. L. Abrams and R. C. Lind, Opt. Lett. 2, 94 (1978).

[5]W. Smith, W. J. Tomlinson, D. J. Eilenberger, and P. T. Moloney, Opt. Lett. 6, 581 (1981).

[6]R. G. Caro and M. C. Gower, Appl. Phys. Lett. 39, 855 (1981), and references therein.

[7]J. R. Salcedo and A. E. Siegman, IEEE J. Quantum Electron. QE-15, 250 (1979); K. A. Nelson and M. Fayer, J. Chem. Phys. 72, 5202 (1980).

[8]B. Fischer, M. Cronin-Golomb, J. O. White, and A. Yariv, Opt. Lett. 6, 519 (1981).
[9]H. Kogelnick, Bell Syst. Tech. J. 48, 2909 (1969).
[10]R. D. Mountain, Rev. Mod. Phys. 38, 205 (1966).
[11]L. Landau and E. Lifshitz, *Fluid Mechanics* (Addison-Wesley, Reading, Mass., 1959).
[12]R. C. Desai and R. Kapral, Phys. Rev. A 6, 2377 (1972).
[13]K. Chiang and M. D. Levenson, Appl. Phys. B 29, 23 (1982).
[14]I. L. Fabelinskii, *Molecular Scattering of Light* (Plenum, New York, 1968), p. 33ff.
[15]Landolt Börnstein, *Numerical Data and Functional Relationships in Science and Technology, Group II* (Springer, Berlin, 1962), Vol. 8, pp. 5—573ff.
[16]K. F. Herzfeld and T. A. Litovitz, *Absorption and Dispersion of Ultrasonic Waves* (Academic, New York, 1959).
[17]J. J. Song, J. H. Lee, and M. D. Levenson, Phys. Rev. A 17, 1439 (1978).
[18]S. Saikan (private communication).